Impact of Geometrical Structures On the Output of Neuronal Models –From Spikes To Bursts

Jianfeng Feng*,** Guibin Li*

*Computational Neuroscience Laboratory, The Babraham Institute, Cambridge CB2 4AT, UK

**COGS, University of Sussex at Brighton, BN1 9QH, UK

jf218@cam.ac.uk http://www.cus.cam.ac.uk/~ jf218

Abstract

What is the difference between the efferent spike train of a neuron with a large soma versus that of a neuron with a small soma? For both the two-compartment integrate-and-fire (IF) model and the Pinsky-Rinzel (PR) model, we use a method we call the decoupling approach, to show that the smaller the soma is, the faster and the more irregularly the neuron fires. Two limiting cases: the soma is much smaller than the dendrite or vise versa, are theoretically investigated. We further conclude, in terms of numerical simulations, that cells falling in between the two limiting cases form a continuum with respect to their firing properties (mean firing time and coefficient of variation of inter-spike intervals). As an application of our approach, we also find that when the soma is small, two-compartment models can be employed as slope detectors. Novel and rigorous results for the calculations of mean first exit time and bursting frequency are also included.

1 Introduction

It is well documented in the literature that the geometrical structure of a neuron considerably contributes to its information processing capacity [25]. However, a fully detailed

model is usually hard to study *theoretically* and, most profoundly, the nonhomogeneous distribution of ionic channels along dendritic trees prevents such an investigation. In order to achieve a better understanding of the function of neuronal morphology, we consider two-compartment neuron models which reflect the minimal geometry of a neuron.

We first present a theoretical approach for how the somatic size affects neuronal output when it receives stochastic inputs from the dendritic compartment. In [32, 30], the authors have addressed a similar problem using numerical simulations where the model receives constant and deterministic input. Here we consider the case that neurons receive random, rather than deterministic inputs. The stochastic part of an input signal might play a functional role in processing information, see for example [5, 16, 20, 35, 24] and references therein. Moreover, studies in [32, 30] are confined to a specific model and numerical simulations, whereas some of our conclusions are obtained for generic two-compartment models using theoretical studies. We find that when the somatic compartment is small, the model tends to burst and the bursting length is totally determined by the activity of dendritic compartment. When the somatic compartment is large, the model can be reduced to a single compartment. Furthermore, we also consider the model with nonconstant, deterministic inputs and find that in this case, the model employs bursting activity to detect the slope of incoming signals.

Here are a few words about our approach–what we call a decoupling approach. Using the elimination method, we could rewrite the two-compartment IF model as a linear, second order ODE, which is a special case of Kramer's equation [34]. From the well known theory of Kramer, we could estimate the first exit time [19]. However, there are two shortcomings to this approach. Firstly it is very difficulty to generalize the conclusions above to more generic two-compartment models such as the Pinsky-Rinzel model. Therefore we still lack a general picture about the behaviour of two compartment models. Secondly, the theory of Kramer is an approximation theory and we have to resort to numerical simulations for checking its validity. Another possible approach (see Lemma 1 in Appendix A) which has the same shortcomings as above is the theory of correlated noise [23]. Due to the reasons above, we propose a novel

approach for studying the behavior of two-compartment models. We first consider the two extreme cases of a very large soma and a very small soma. We can easily understand the behaviour for these two cases. With a large soma, the two-compartment model is reduced to a one-compartment model; with a small soma the two-compartment model exhibits bursting behaviour. Bursting has recently been proposed as a possible way of processing information in the cortex [28, 22] and is widely observed in experiments. The results above allow us to develop a rigorous theory about the two-compartment IF model and to calculate the mean firing time and bursting frequency.

2 Models

Let us assume that a neuron is composed of two compartments: a somatic compartment and dendritic compartment. Suppose that a cell receives EPSPs at q_E excitatory synapses and IPSPs at q_I inhibitory synapses and that $V_d(t)$ is the membrane potential of the dendritic compartment at time t. When the somatic membrane potential $V_s(t)$ is between the resting potential V_{rest} and the threshold V_{thre},

$$\begin{cases} dV_s(t) &= -\dfrac{1}{\gamma}(V_s(t) - V_{rest})dt + g_c\dfrac{V_d(t) - V_s(t)}{p}dt \\ dV_d(t) &= -\dfrac{1}{\gamma}(V_d(t) - V_{rest})dt + g_c\dfrac{V_s(t) - V_d(t)}{1-p}dt + \dfrac{di_{syn}(t)}{1-p} \end{cases} \tag{2.1}$$

where $1/\gamma$ is the decay rate and p is the ratio between the membrane area of the somatic compartment and the whole cell. $g_c > 0$ is a constant, and the synaptic input is

$$i_{syn}(t) = a\sum_{i=1}^{q_E} dE_i(t) - b\sum_{j=1}^{q_I} dI_j(t)$$

where $E_i(t), I_i(t)$ are Poisson processes with rates λ_E and λ_I respectively and a, b are the magnitudes of each EPSP and IPSP. After $V_s(t)$ crosses V_{thre} from below, a spike is generated and $V_s(t)$ is reset to V_{rest}. This model is called the two-compartment integrate-and-fire model. The interspike interval of efferent spikes is

$$T(p) = \inf\{t : V_s(t) \geq V_{thre}\}$$

for $1 > p > 0$. It is well known that Poisson input can be approximated by

$$I_{syn}(t) = \mu t + \sigma B_t$$

where B_t is the standard Brownian motion, $\mu = aq_E\lambda_E - bq_I\lambda_I$ and $\sigma = \sqrt{a^2q_E\lambda_E + b^2q_I\lambda_I}$. Thus, Eq. (2.1) now becomes

$$\begin{cases} dV_s(t) &= -\frac{1}{\gamma}(V_s(t) - V_{rest})dt + g_c\frac{V_d(t) - V_s(t)}{p}dt \\ dV_d(t) &= -\frac{1}{\gamma}(V_d(t) - V_{rest})dt + g_c\frac{V_s(t) - V_d(t)}{1-p}dt + \frac{dI_{syn}(t)}{1-p} \end{cases} \tag{2.2}$$

In the following, we consider the two-compartment IF model to be the model defined by Eq. (2.2).

We also consider a simplified, two-compartment biophysical model, proposed by Pinsky and Rinzel [32]. They have demonstrated that the model mimics a full, very detailed Traub model quite well.

The Pinsky-Rinzel model is defined by

$$\begin{cases} C_m dV_s(t) &= -I_{Leak}(V_s)dt - I_{Na}(V_s,h)dt - I_{K-DR}(V_s,n)dt + g_c\frac{V_d(t) - V_s(t)}{p}dt \\ C_m dV_d(t) &= -I_{Leak}(V_d)dt - I_{Ca}(V_d,s)dt - I_{K-AHP}(V_d,q)dt - I_{K-C}(V_d,Ca,c)dt \\ & \quad + \frac{dI_{Syn}}{1-p} + g_c\frac{V_s(t) - V_d(t)}{1-p}dt \\ Ca' &= -0.002I_{Ca} - 0.0125Ca \end{cases} \tag{2.3}$$

In our calculations, all parameters and equations are identical to those used in [32] except for the parameters of the calcium equation which are from [38].

3 Analytical Results

In this section we consider two limiting cases–soma of infinitely small size, and the limit of small dendrite. For these two cases analytical results are derived that give the mean interspike intervals as well as the variance and the CV (defined below). The analysis implies that neurones with small soma fires more irregularly than neurones with a large soma. Also small soma models show intermittent bursting, the inter-burst intervals and burst lengths are calculated.

Without loss of generality, we assume that $g_c = 1$ in this section. For the two-compartment IF model, it is trivial to determine the mean and standard variation of the *membrane potential* of the somatic compartment. However, these values provide insight for understanding the behaviour of the model.

A detailed calculation of the mean and variance of the membrane potential is presented in Appendix A. After omitting all terms of $o(t)$, we conclude from Eq. (7.3) and (7.4) that

$$\langle V_s \rangle = \frac{\mu\gamma^2}{p(1-p)+\gamma} \tag{3.1}$$

and

$$\langle (V_s - \langle V_s \rangle)^2 \rangle = \frac{\sigma^2\gamma^3}{2[p(1-p)+\gamma][2p(1-p)+\gamma]} \tag{3.2}$$

When $p = 0.5$, both the mean and variance of the membrane potential of the somatic compartment reach their minimal values. One might thus conclude that the mean and variance of efferent interspike intervals, or at least the mean, should exhibit similar behaviour: i.e. attain their minimal value when $p = 0.5$. However, that is not the case due to the memory in the model (see next section)[1].

Let us now consider a generic two-compartment model defined by

$$\begin{cases} dV_s(t) &= f(V_s, V_d)dt + \dfrac{V_d(t) - V_s(t)}{p}dt \\ dV_d(t) &= g(V_s, V_d)dt + \dfrac{V_s(t) - V_d(t)}{1-p}dt + \dfrac{dI_{syn}(t)}{1-p} \end{cases} \tag{3.3}$$

where f, g are two functions. Eq. (3.3) certainly includes the Pinsky-Rinzel model as a special case.

Consider the case where $p \to 0$. Multiplying both sides of the equation for the somatic compartment by p and taking $p \to 0$, we see that $V_d = V_s$ (for the existence of the limit, we refer the reader to Appendix B. At the same time the equation for the dendritic compartment becomes

$$dV_d = g(V_s, V_d)dt + dI_{syn}(t) = g(V_d, V_d)dt + dI_{syn}(t) \tag{3.4}$$

[1] In Appendix A, we assume that $V_s|_{t=0} = V_d|_{t=0} = 0$

since $p \to 0$ and $V_d = V_s$. Similarly for the case where $p \to 1$. Multiplying both sides of the equation for the dendritic compartment by $1-p$ and taking $p \to 1$, we see that $V_d - V_s = I_{syn}$. At the same time the equation for the somatic compartment becomes

$$dV_s = f(V_s, V_s + I_{syn})dt + dI_{syn}(t) \tag{3.5}$$

Therefore we have the following two cases

- When $p \to 1$, V_s is defined by the following equation

$$dV_s = f(V_s, V_s + I_{syn})dt + dI_{syn}(t) \tag{3.6}$$

- When $p \to 0$, $V_s = V_d$ and V_d is given by the following equation

$$dV_d = g(V_d, V_d)dt + dI_{syn}(t) \tag{3.7}$$

We emphasize that the derivation of Eq. (3.6) and Eq. (3.7) is independent of the concrete form of synaptic inputs. Hence the conclusions hold true for neuromudulator based inputs, such as AMPA, NMDA, GABA_A and GABA_B [6].

When Eq. (3.3) is the two-compartment IF model and t is large enough, we then conclude that[2] $V_s(t)$ for $p = 1$ is equal to $V_s(t)$ for $p = 0$ since Eq. (3.6) is identical to Eq. (3.7). We note that in Eq. (7.3) and Eq. (7.4), both the mean and the variance are equal for $p = 0$ and $p = 1$. Thus the results of Eq. (3.6) and (3.7) are agree with the conclusions of Lemma 1 in Appendix A.

The conclusion of Eq. (3.6) and (3.7) is very illuminating. Consider, for example, the two-compartment IF model.

- When $p \to 1$, according to Eq. (3.6) and (3.7), we conclude that the two-compartment model behavior is the same as the behavior of the conventional IF model which is well studied in the literature [3, 4, 10, 11, 14, 15, 17, 18]. When $\gamma\mu > V_{thre}$, the output spike trains are generally regular with a coefficient

[2] We use $p = 1$ and $p = 0$ for $\lim_{p\to 1}$ and $\lim_{p\to 0}$

of variation (CV) smaller than 0.5. In this case, instances where the threshold is crossed are mainly due to deterministic forces. When $\gamma\mu < V_{thre}$ then the output spike trains are irregular with a coefficient of variation (CV) greater than 0.5. In this case threshold crossings are primarily due to random fluctuations.

- When $p \to 0$, the somatic membrane potential is identical to that of the dendritic compartment. Suppose that $V_d(t) > V_{thre}$ for $t \in [t_0, t_1]$. Then $V_s(t)$ will fire very fast during $[t_0, t_1]$. In theory, it fires with an infinite frequency. This can not happen as a real neuron which has a refractory period. On the other hand, if $V_d(t) < V_{thre}$ for $t \in [t_0, t_1]$, then $V_s(t) = V_d < V_{thre}$, and the neuron is silent. The analyses above for $p = 0$ give rise to bursting behaviour. During the interval $[t_0, t_1]$, when $V_d > V_{thre}$, the cell fires with a very high frequency; while, when $[t_0, t_1]$ with the property that $V_d < V_{thre}$, the cell is completely silent.

Similar arguments can be applied to Pinsky-Rinzel model. When $p \to 1$, the model is reduced to a somatic compartment. When $p \to 0$, if the neuron fires, it will fire with its highest possible frequency, provided that $V_d(t)$ is greater than the threshold of the somatic compartment membrane potential (see Section 5, in particular Fig. 6).

For the case of small p, it is not very informative to calculate the interspike intervals. It is more interesting to consider the inter-burst intervals T_i and burst length T_l. According to our results above, when $p \to 0$,

$$\begin{cases} T_i &= \sup\{t : V_0 = V_{thre}, V_d(s) \le V_{thre}, \text{ for } 0 \le s \le t\} \\ T_l &= \sup\{t : V_0 = V_{thre}, V_d(s) \ge V_{thre}, \text{ for } 0 \le s \le t\} \end{cases} \tag{3.8}$$

Note that the cases where V_s for $p = 1$ and V_d for $p = 0$ are very different when t is small, although they appear to be identical. V_s for $p = 1$ is not a stationary process, but V_d for $p = 0$ is a stationary process.

Combining the arguments above and defining

$$CV(p) = \sqrt{\langle T(p)^2 - (\langle T(P)\rangle)^2\rangle}/\langle T(p)\rangle,$$

we arrive at the following conclusions.

For the two-compartment IF model, we have

$$P(B_i)\langle T_i\rangle = \langle T(0)\rangle < \langle T(1)\rangle, \text{ and } CV(0) > CV(1) \tag{3.9}$$

where a rigorous and analytical expression of $\langle T(1)\rangle$ is presented in the following and $B_i = \{V_d(0) = V_{thre}, \frac{dV_d}{dt}|_{t=0} < 0\}$

Numerical examples for $0 < p < 1$ are included in the next section. In the following we discuss the cases of $p = 1$ and $p = 0$ separately.

When $p = 1$, we consider the conventional, one-compartment IF model. An analytical expression for the mean interspike intervals of the IF model has been obtained in terms of the solution of PDEs, as shown in [31, 33, 37]. However, such a formula usually involves some special functions and is in general not very informative and various approximations have to be found. In Appendix C we present a rigorous, and analytical approach for calculating the mean firing time, which could be applied to any one dimensional neuron model. Examples are the integrate-and-fire model, the θ-neuron [7] and the IF-FHN model [19], although here we confine ourselves to the IF model.

Applying Theorem 1 in Appendix C to the IF model, we obtain

$$\begin{aligned}\langle T(1)\rangle &= \frac{2}{\sigma^2}[\int_{V_{rest}}^{V_{thre}} \exp(\frac{(x-\gamma\mu)^2|_{V_{rest}}^{y}}{\sigma^2\gamma})dy] \cdot [\int_{-\infty}^{V_{rest}} \exp(-\frac{(x-\gamma\mu)^2|_{V_{rest}}^{y}}{\sigma^2\gamma})dy] \\ &+\frac{2}{\sigma^2}\int_{V_{rest}}^{V_{thre}} [\int_{y}^{V_{thre}} \exp(\frac{(x-\gamma\mu)^2|_{V_{rest}}^{u}}{\sigma^2\gamma})du] \exp(-\frac{(x-\gamma\mu)^2|_{V_{rest}}^{y}}{\sigma^2\gamma})dy\end{aligned} \tag{3.10}$$

Note that it is easier to numerically calculate the mean firing time using Eq. (3.10) than using the method in [37]. From Eq. (3.10) we see that when $V_{thre} < \gamma\mu$, $\langle T(1)\rangle \to 0$ as $\sigma \to 0$; when $V_{thre} > \gamma\mu$, $\langle T(1)\rangle \to \infty$ as $\sigma \to 0$. In terms of Eq. (3.10), we could further calculate, for example, the Fish information etc. and we will discuss it in subsequent publications.

Now we turn to the case where $p = 0$. Solving the equation for the dendritic compartment, we obtain

$$V_d(t) - \gamma\mu(1 - \exp(-t/\gamma)) = V_d(0)\exp(-t/\gamma) + \sigma\int_0^t \exp(-(t-s)/\gamma)dB_s$$

Its covariance function is given by

$$r(\tau) = \frac{\sigma^2\gamma}{2}\exp(-|\tau|/\gamma)$$

for $\tau \in I\!R$. The burst frequency is identical to the upcrossing of V_{thre} for the stationary process V_d. By a direct application of Rice's formula (see [29]), we obtain the following conclusions.

The bursting frequency is given by

$$\frac{1}{2\pi}\sqrt{|r''(0)|}\exp(-\frac{(V_{thre}-\gamma\mu)^2}{2}) = \frac{\sigma}{2\pi\sqrt{\gamma}}\exp(-\frac{(V_{thre}-\gamma\mu)^2}{2})$$

Furthermore, using large deviation theory [1, 19, 21], we could estimate the mean interbursting intervals T_i when $V_{thre} > \gamma\mu$ and mean burst length T_l when $V_{thre} < \gamma\mu$. The obtained results are approximations and so we do not present them here. A rigorous and exact estimate would be of interest.

We emphasize that there would never be a case where $p = 0$ or $p = 1$. All our conclusions above are true for p sufficiently close to zero or p sufficiently close to one. However the decoupling approach helps us gain a better understanding of the model behaviour and therefore develop a theory for studying the model. In the next section we consider models and behavior between these two extreme cases.

4 Numerical Results

In this section, for both the integrate-and-fire model and the Pinsky-Rinzel model, we are going to show that cells falling in between the two limiting cases (large soma or large dendrite as discussed in the previous section) form a continuum with respect to their firing properties (mean and CV), i.e. for CV and mean firing time, the gap between $p = 0$ and $p = 1$ is filled in a monotone manner with respect to p.

We simulate the two-compartment IF model and the Pinsky-Rinzel model with the following synaptic parameters: $a = b = 0.5mV, \lambda_E = 100Hz, \lambda_I = 0, 10, \cdots, 100Hz, q_E = q_I = 100$. The threshold for detecting a spike for both the

soma and dendrite of the Pinsky-Rinzel model is 30mV and $g_c = 2.1$. In the two-compartment IF model, we let $V_{rest} = 0., V_{thre} = 20mV, \gamma = 20.2$ and $g_c = 4$.

Numerical results for the membrane potentials of the somatic and dentritic compartments of the two-compartment IF model are presented in Fig. 1 and Fig. 2 for $p = 0.95$ and $p = 0.05$ respectively with $\lambda_I = 80$Hz. As we have discussed in the previous section, when $p = 0.95$ the model behaviour approximates a single compartment model behaviour; when $p = 0.05$, the model bursts and the bursting behaviour is determined by V_d without coupling.

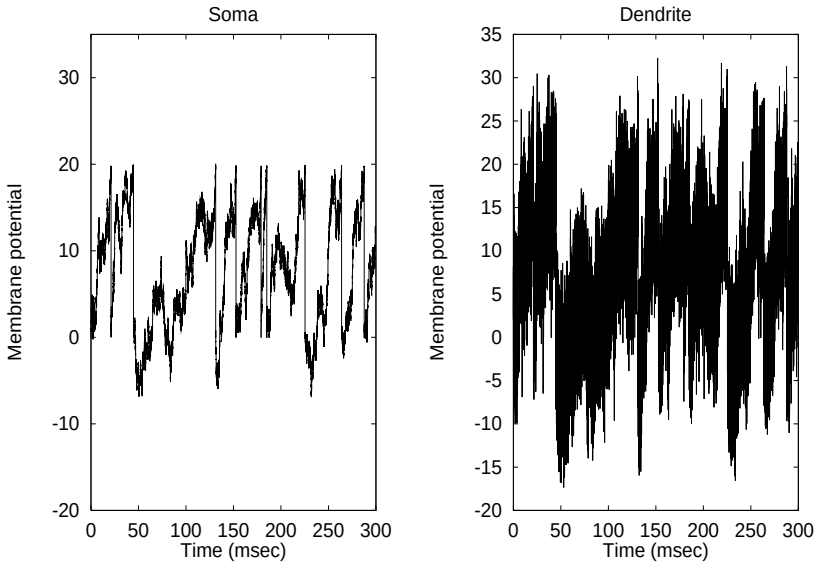

Figure 1: Membrane potential of the two-compartment IF model with $p = 0.95$.

For the two-compartment IF model, as shown in Fig. 3, we see that both the mean firing frequency and the CV are increasing functions of p. Therefore the gap between $p = 0$ and $p = 1$ described in the previous section is filled in a monotone manner with respect to p. The meaning firing time for $p = 0.5$ does not attain the maximum (see Lemma 1).

We also note that when $p = 1$, efferent spike trains are very irregular even when inputs are exclusively excitatory. As we pointed out in the previous section, when p is small, the CV of efferent spike trains is quite high.

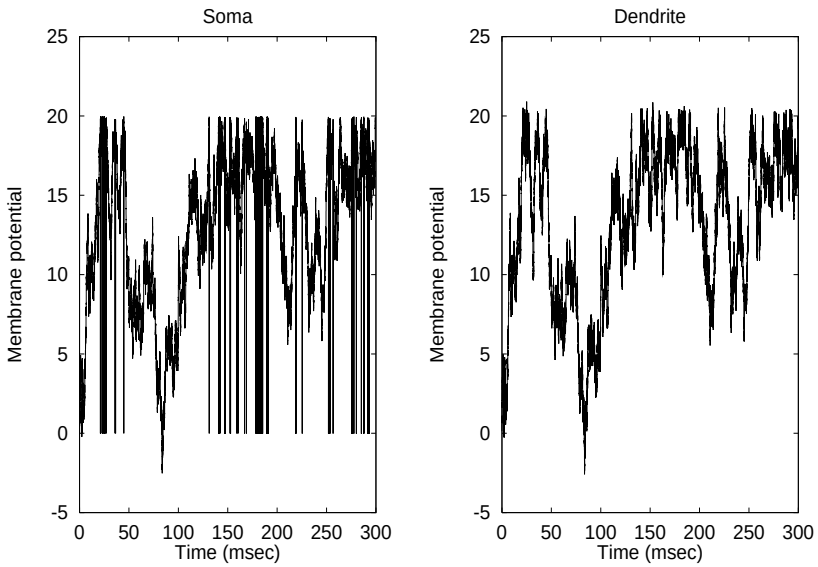

Figure 2: Membrane potential of the two-compartment IF model with $p = 0.05$. Note that the membrane potentials of the soma and the dendrite are almost identical, except the reset of the somatic compartment. Compare with Fig. 1.

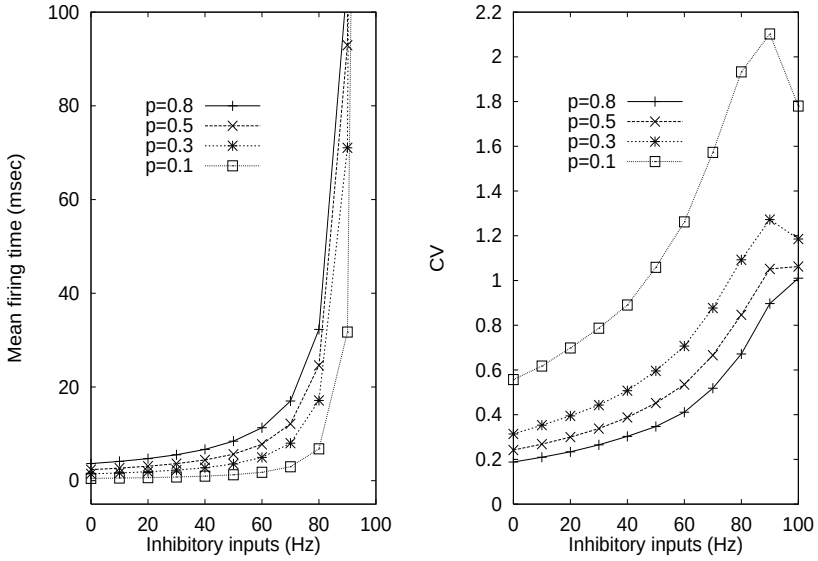

Figure 3: Mean firing time and CV vs. λ_I for $p = 0.1, 0.3, 0.5, 0.8$ for the two-compartment IF model. 10000 spikes are generated for calculating the mean firing time and CV. Parameters are specified in the context.

For the Pinsky-Rinzel model, behaviour similar to that of the IF model is observed. The gap between $p = 0$ and $p = 1$ is filled in a monotone way (Fig. 4) with respect to p. As we adjust the geometrical parameter p, the model exhibits a variety of behaviour.

In conclusion, we have obtained a complete picture of the behavior of these two-compartment models. Both mean firing time and CV are monotone function of p where p is the ratio of the somatic compartment area with respect to the whole cell.

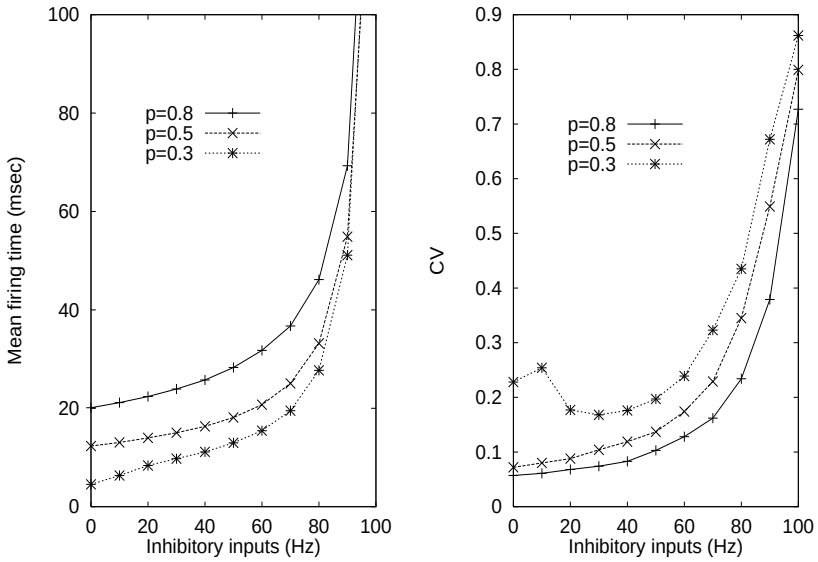

Figure 4: Mean firing time and CV vs. λ_I for the Pinsky-Rinzel model with $p = 0.3, 0.5, 0.6$. 10000 spikes are generated for calculating the mean firing time and CV. Parameters are specified in the context.

5 Bursting as a Slope Detector

In the previous sections we discussed the details of the behaviour of two-compartment models. In particular, we showed that when p is small, the neuron bursts when the dendritic membrane potential is above the threshold. In recent years, there have been many research activities devoted to the topic of how a neuron processes information via bursting [28, 22], rather than via individual spikes. In particular, there is both

experimental and modeling evidence, that suggests that bursting activity might be employed by neurons as a way of detecting the slope of incoming signals. As an application of the results in the previous sections, let us consider the two-compartment IF model with synaptic inputs defined by

$$dI_{syn}(t) = \mu dt + \cos(\omega t)dt \tag{5.1}$$

where $\omega > 0$. For simplicity of notation we assume that $\mu\gamma = V_{thre}$.

Solving the linear equation

$$dV_d = -\frac{V_d}{\gamma}dt + dI_{syn}(t)$$

with initial condition $V_d(0) = 0$ and omitting higher order terms containing $\exp(-t/\gamma)$, we obtain

$$V_d = V_{thre} + \gamma \sin(\omega t + \phi) \tag{5.2}$$

where $\sin(\phi) = 1/(1 + \omega^2\gamma^2)$. According to our conclusions in the previous sections, when p is small the neuron will fire with a high frequency (bursting) whenever $\sin(\omega t + \phi) > 0$, and will be completely silent if $\sin(\omega t + \phi) < 0$. Assume that ϕ is small enough so that $\{t : \sin(\omega t + \phi) > 0\}$ corresponds to the decreasing part of $\cos(\omega t)$. Then when p is small, the two-compartment IF model is naturally a slope detector, via bursting activities. The presence of ϕ, a phase lag, in Eq. (5.2) is a natural constrain for the model behaviour.

When p is large, the model is reduced to the IF model and which has been well studied in the literature [26].

In general for the synaptic input

$$dI_{syn}(t) = s(t)dt \tag{5.3}$$

where $s(t) \in C^\infty$, we know that busting could be a detector of the following set

$$\{t : \gamma s(t) - \gamma^2 s'(t) + \gamma^3 s''(t) - \cdots - V_{thre} \geq 0\}$$

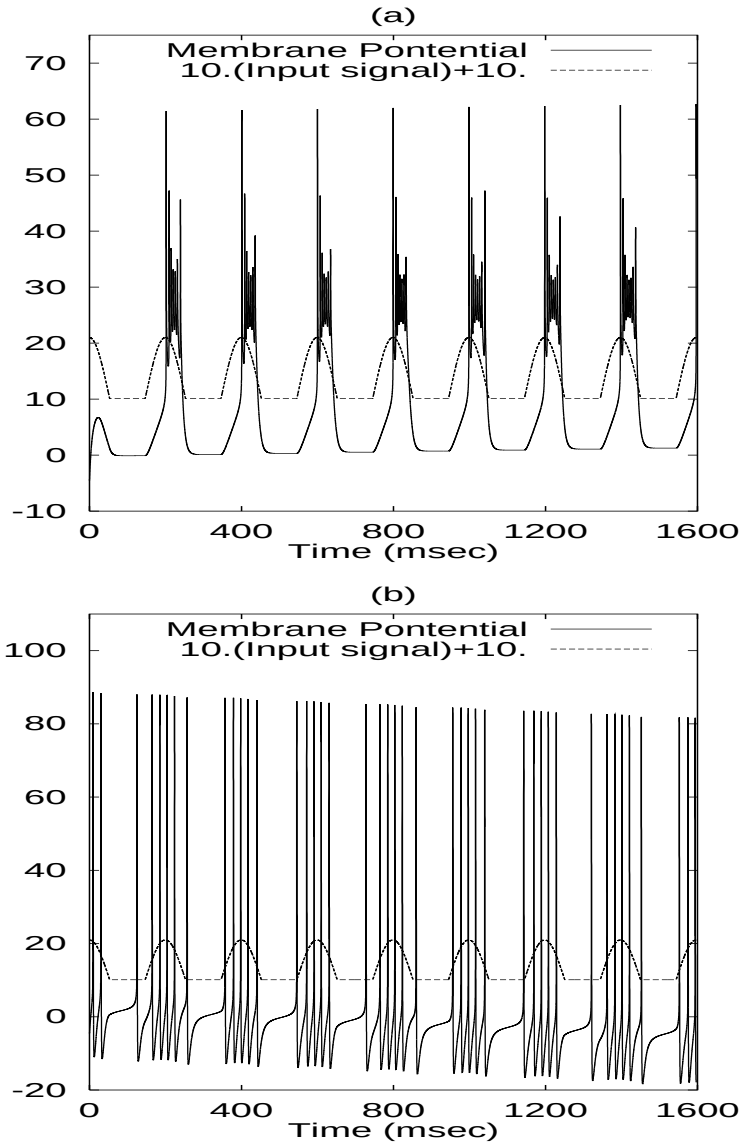

Figure 5: Membrane potentials of the somatic compartment of the Pinsky-Rinzel model with input signal $dI_{syn}/dt = max(\cos(2\pi t/200.) + 0.1, 0)$. (a) Note that the model bursts when the input signal decreases in the case where $p = 0.1$, and therefore it is a slope detector. (b) When $p = 0.9$, the neuron fires when it receives a strong signal.

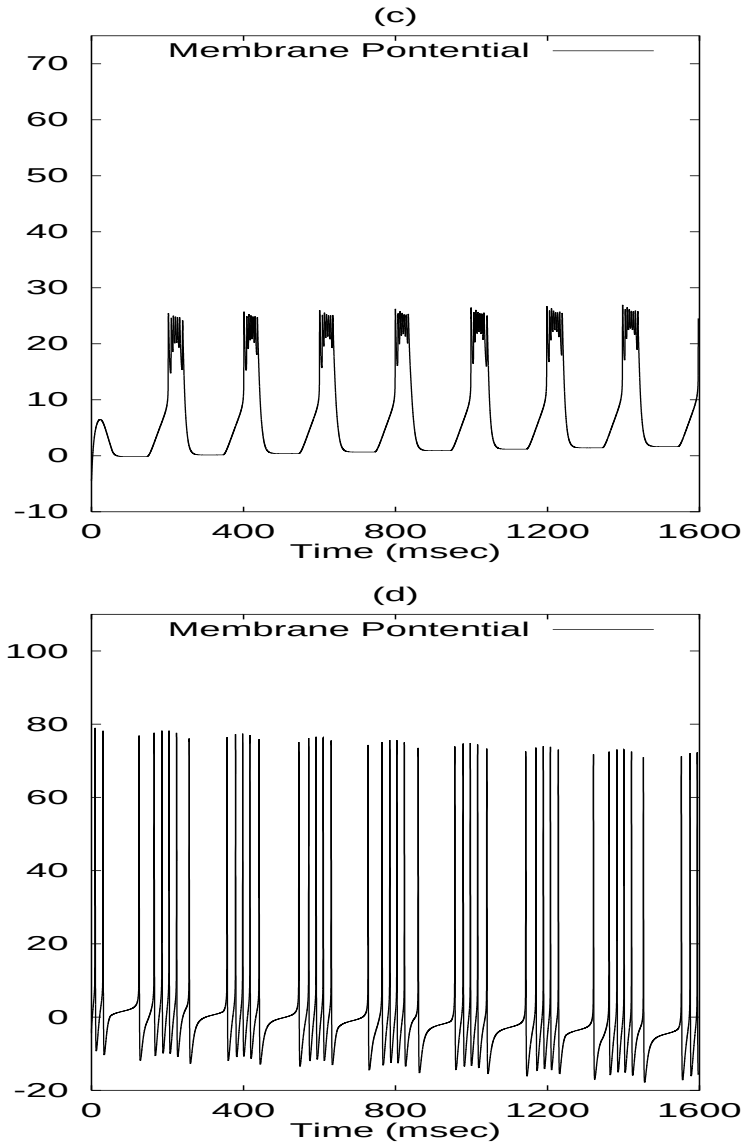

Figure 6: (Continuous of Fig. 5) Membrane potentials of the dendritic compartment of the Pinsky-Rinzel model with input signal $dI_{syn}/dt = max(\cos(2\pi t/200.) + 0.1, 0)$. (c) $p = 0.1$, compare with (a). It is easily seen that the membrane potential of the dendritic compartment and somatic compartment is identical before bursting. Bursting is due to the fact that the membrane potential of the dendritic compartment crosses the threshold of the somatic compartment, as we discussed in the previous section. (d) The membrane potential of the dendritic compartment when $p = 0.9$, compare with (b).

To further demonstrate our theory above, we simulate the Pinsky-Rinzel model with input

$$\frac{dI_{syn}}{dt} = max(\cos(2\pi t/200.) + 0.1, 0)$$

Fig 5 shows simulation results for parameters $g_{K-DR} = 21, g_{Na} = 35, p = 0.1$ and $p = 0.9$. All other parameters are the same as in the previous section. Then $p = 0.1$, the model responds to input signals by emitting bursts. Note that the model bursts only when the input signal decreases, i.e. its slope is negative. When $p = 0.9$ the phenomena are not observable at all. It is interesting to note that although the theoretical results above are obtained for a linear model(before resetting) we could generalize it to nonlinear, biophysical models such as the PR model. It seems that the linear theory is widely 'used' by neurons, see for example [8]. Furthermore, we point out that the fact that the neuron bursts at the decreasing phase of incoming signals is not trivially due to the delay of neuronal response. In fact, Fig. 5 indicates that when the incoming signals reach their minima, the membrane potentials of the somatic compartment also attain their global minima with a delay much shorter than the burst length.

We further test the stability of the neuronal response by modifying the input signal as follows

$$\frac{dI_{syn}}{dt} = max(\cos(2\pi t/200.) + 0.1 + \xi, 0)$$

where ξ is normally distributed with mean zero and variance one. Even though the noise level is quite high, compared to the input signal, the model shows a very reliable behaviour as shown in Fig. 7.

6 Discussion

We have considered the behaviour of two-compartment models, as a first step to understanding the impact of the geometrical structures of neurons on their input-output relationship. We find that when the somatic compartment is large, a two-compartment model can be reduced to a single one-compartment model. When the somatic com-

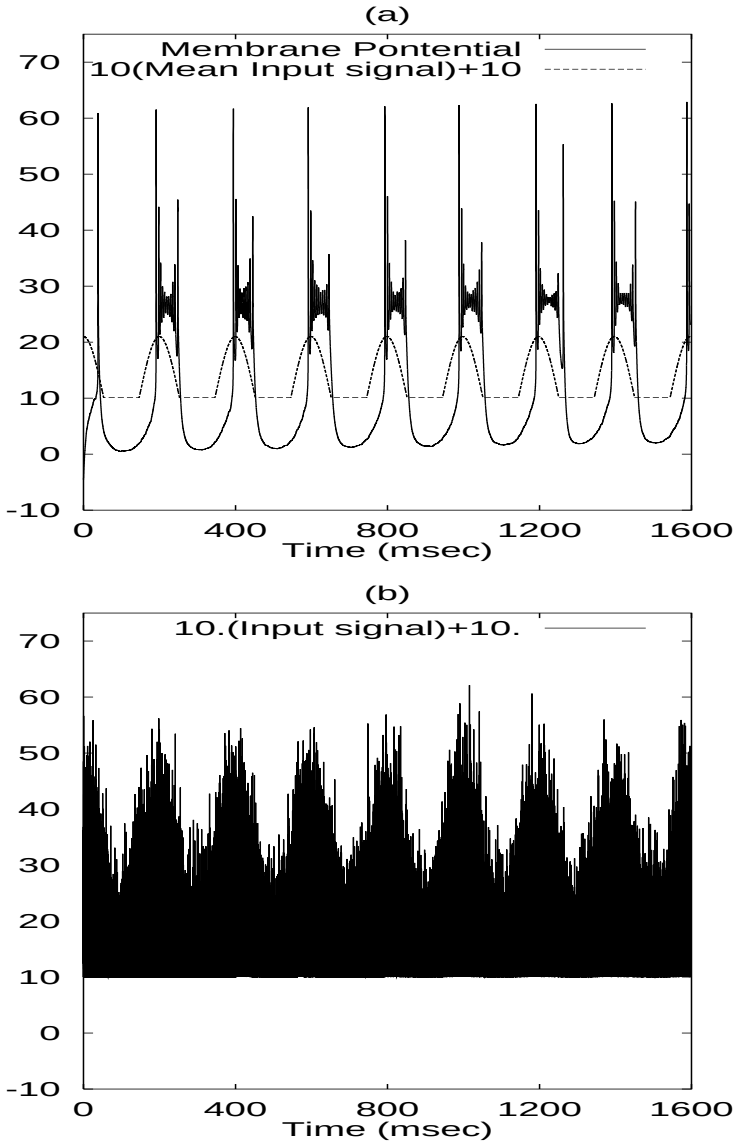

Figure 7: Membrane potentials of the somatic compartment of the Pinsky-Rinzel model with input signal=$dI_{syn}/dt = max(\cos(2\pi t/200.) + 0.1 + \xi, 0)$ as defined in the text where $p = 0.1$. (a) The model bursts when the input signal decreases. (b) Input signal perturbed by noise, i.e. $max(\cos(2\pi t/200.) + 0.1 + \xi, 0)$.

partment is small, it exhibits bursting behaviour and its behaviour is determined by the activity of the dendritic compartment alone. Therefore in each case the original, coupled two-compartment model is reduced to a single compartment model which we call the decoupling approach. By a combination of theoretical analyses and numerical simulations, we conclude that both the first and second order statistics (mean and CV) of interspike intervals are monotone functions of the somatic size. We then present theoretical results for calculating the mean interspike intervals and burst frequencies.

We also conclude that when the somatic size is small two-compartment models function as slope detectors for incoming signals, i.e. when the input signal decreases the model bursts and is silent otherwise.

Finally we briefly discuss the biological implications of changing p–what we call global plasticity. Subcellular morphology changes have been reported recently in a few type neurones [2, 9]. The most striking and direct example of global plasticity is from vasopressin and oxytocin cells in the supraoptic and paraventricular nulcei. For both type neurons it is found that p changes during lactation [36]. For example, in the oxtocin cell a shrinkage of the dendritic tree and an enlargement of the soma is observed, accompanying by a considerable change in the electrical properties of the neuron. In the classical approach of learning theory, the Hebb learning rule plays an essential role. Based upon it, many models are developed [12, 13]. The Hebb learning rule is a local plasticity principle where increasing the activities both presynaptically and the postsynaptically induces an increase in the strength of *this* synapse. Due to the large number on synapses of each neuron, the functional consequence of the modification of the strength of a single synapse is bound to be limited. In contrast a global change of the neuronal morphology [3] would be *a* much more efficient way to modify the input-output relationship. As we demonstrate here, both theoretically and numerically, an increase or a decrease in p alone causes a neuron to behave completely different where both firing rate and the firing pattern (CV) vary. Furthermore, we have not taken into account the effect of input modifications due to the pruning or elaboration of dendritic

[3]Here we do not exclude the possibilities that modifying cell's biophysical properties can result in similar effects as morphology changes.

trees, as reported in experiments [36], which will more dramatically modify the input-output relationship. Several challenging problems remain. We must determine whether global plasticity can be observed experimentally in other neurons and if so, for which stimuli the global plasticity occurs. We may also be able to apply global plasticity to the design of artificial neural networks that achieve a more powerful and efficient learning. It would also be interesting to consider how changing p on the synchronization properties of a group of neurons [16].

Acknowledgement. We are grateful to anonymous referees for their valuable comments on an earlier version of this manuscript, and to D. Brown, B. Ermentrout, P. Lansky, P. Roper and A. Sherman for their discussions, J.F. is also to Prof. W. Rall for his encouragement to work on two-compartment models. The work was partially supported by BBSRC and an ESEP grant of the Royal Society.

References

[1] Albeverio, S., Feng, J., and Qian M. (1995) Role of noises in neural networks *Phys. Rev. E.* **52** 6593-6606.

[2] Andersen P. (1999), A spine to remember *Nature*, **399** 19-21.

[3] Brown D., and Feng J. (1999) Is there a problem matching model and real CV(ISI)? *Neurocomputing* **26-27**, 117-122.

[4] Brown D., Feng J., and Feerick S.(1999) Varibility of firing of Hodgkin-Huxley and FitzHugh-Nagumo neurons with stochastic synaptic input. *Phys. Rev. Lett.* **82** 4731-4734.

[5] Collins J.J., Chow, C.C., and Imhoff T.T. (1995) Stochastic resonance without tuning. *Nature* **376** 236-238.

[6] Destexhe A., Mainen Z.F., and Sejnowski T.J. (1998) Kinetic models of synaptic transmittion. C. Koch and I. Segev eds. *Methods in Neuronal Modeling* The MIT Press: Cambridge Massachusetts.

[7] Ermentrout, B. (1996) Type I membranes, phase resetting curves, and synchrony. *Neural Compuatation* **8** 979-1001.

[8] Ermentrout, B. (1998) Linearization of F-I curves by adaptation *Neural Compuatation* **10** 1721-1729.

[9] Engert F., and Bonhoeffer T. (1999) Dendritic spine changes associated with hippocampal long-term synaptic plasticity. *Nature* **399** 66-70.

[10] Feng, J.(1997), Behaviours of spike output jitter in the integrate-and-fire model. *Phys. Rev. Lett.* **79** 4505-4508.

[11] Feng, J. (1999). Origin of firing varibility of the integrate-and-fire model *Neurocomputing* **26-27** 87-91.

[12] Feng J., Pan H., and Roychowdhury V. P. (1996). On neurodynamics with limiter function and Linsker's developmental model. *Neural Computation* **8**, 1003-1019.

[13] Feng J., Pan H., and Roychowdhury V. P. (1997). Linsker-type Hebbian learning: a qualitative analysis on the parameter space. *Neural Networks* **10**, 705-720.

[14] Feng J., and Brown D.(1998). Spike output jitter, mean firing time and coefficient of variation, *J. of Phys. A: Math. Gen.*, **31** 1239-1252.

[15] Feng J, and Brown D. (1998). Impact of temporal variation and the balance between excitation and inhibition on the output of the perfect integrate-and-fire model *Biol. Cybern.* **78** 369-376.

[16] Feng J., Brown D., and Li G.(2000). Synchronisation due to common pulsed input in Stein's model *Phys. Rev. E*, **61** 2987-2995.

[17] Feng J., and Brown D.(1999). Coefficient of variation greater than .5 how and when? *Biol. Cybern.* **80**, 291-297.

[18] Feng J., and Brown D.(2000). Impact of correlated inpus on the output of the integrate-and-fire models *Neural Computation* **12** 711-732.

[19] Feng J., and Brown D.(2000) Integrate-and-fire models with nonlinear leakage *Bulletin of Mathematical Biology*(in press)

[20] Feng, J., and Tirozzi B. (2000) Stochastic resonance tuned by correlations in neuronal models. *Phys. Rev. E.* (in press, April).

[21] Freidlin M.I., and Wentzell A.D. (1984) *Random Perturbations Of Dynamical Systems*, Springer-Verlag: New York.

[22] Metzner,W, Koch,C, Wessel,R, and Gabbiani,F(1998) Feature extraction by burst-like spike patterns in multiple sensory maps *J. Neuroscience* **18** 2283-2300.

[23] Hänggi P., and Jung P.(1995) Colored noise in dynamical systems *Advances in Chemical Physics,* eds. Prigogine I., and Rice S.A., John Wiley & Sons Inc.

[24] Harris, C.M., and Wllpert, D.M., (1998) Signal-dependent noise determines motor planning, *Nature* **394** 780-783.

[25] Koch, C. (1999) *Biophysics of Computation*, Oxford University Press.

[26] Keener J.P., Hoppensteadt F.C., and Rinzel J. (1981) Integrate and fire models of nerve membranes response to oscillatory inputs. *SIAM J. Appl. Math.* **41** 503-517.

[27] Karlin S. and Taylor H.M. (1982) *A Second Course in Stochastic Processes* Academic Press, New York.

[28] Lisman J.E. (1997) Bursts as a unit of neural informaiton: making unreliable synapses reliable. *Trends in Neuroscience* **20** 38-43.

[29] Leadbetter, M.R., Lindgren, G., and Rootzén, H. (1983) *Extremes and Related Properties of Random Sequences and Processes.* Springer-Verlag, New York, Heidelberg, Berlin.

[30] Mainen Z.F., and Sejnowski, T. J.(1996). Influence of dendritic structure on firing pattern in model neocortical neuron *Nature* **382** 363-366.

[31] Musila M., and Lánský P.(1994). On the interspike intervals calculated from diffusion approximations for Stein's neuronal model with reversal potentials, *J. Theor. Biol.* **171**, 225-232.

[32] Pinsky, P.F., and Rinzel J. (1994) Intrinsic and network rhythmogensi in a reduced Traub model for CA3 neurons, *J. Computational Neuroscience* **1** 39-60.

[33] Ricciardi, L.M., and Sato, S.(1990), Diffusion process and first-passage-times problems. *Lectures in Applied Mathematics and Informatics* ed. Ricciardi, L.M., Manchester: Manchester University Press.

[34] Risken, S. (1989). *The Fokker-Planck Equation* Springer-Verlag: Berlin etc.

[35] Sejnowski, T.J.(1998) Making smooth moves *Nature 394* 725-726.

[36] Stern J.E., and W.E. Armstrong (1998) Reorganization of the dentritic trees of oxytocin and vasopressin neurons of the rat supraoptic nucleus during lactation. *J. Neuroscience* **18** 841-853.

[37] Tuckwell H. C. (1988), *Stochastic Processes in the Neurosciences.* Society for industrial and applied mathematics: Philadelphia, Pennsylvania.

[38] Wang X.J. (1998) Calcium coding and adaptive temporal computation in cortical pyramidal neurons. *J. Neurophysiol.* **79** 1549-1566.

7 Appendix A

Assuming $V_s|_{t=0} = V_d|_{t=0} = 0$, we solve the linear equation for the two-compartment IF model

$$\begin{cases} V_s - V_d &= -\dfrac{\mu\gamma p(1-e^{(\frac{1}{\gamma}+\frac{1}{p(1-p)})t})}{p(1-p)+\gamma} - \dfrac{\sigma}{1-p}\displaystyle\int_0^t e^{-(\frac{1}{\gamma}+\frac{1}{p(1-p)})(t-x)}dB_x \\ V_s + V_d &= \dfrac{\gamma\mu p + 2\gamma^2\mu}{p(1-p)+\gamma} - 2\gamma\mu e^{-\frac{t}{\gamma}} + \dfrac{p(1-2p)\gamma\mu}{p(1-p)+\gamma}e^{-(\frac{1}{\gamma}+\frac{1}{p(1-p)})t} \\ & \quad + \dfrac{(1-2p)\sigma}{p(1-p)^2}\displaystyle\int_0^t e^{-\frac{t-x}{\gamma}}\int_0^x e^{-(\frac{1}{\gamma}+\frac{1}{p(1-p)})(x-y)}dB_y dx + \dfrac{\sigma}{1-p}\int_0^t e^{-\frac{t-x}{\gamma}}dB_x \end{cases} \tag{7.1}$$

Therefore

$$\begin{aligned} V_s &= \frac{\mu\gamma^2}{p(1-p)+\gamma} - \mu\gamma e^{-\frac{t}{\gamma}} + \frac{\mu\gamma p(1-p)}{p(1-p)+\gamma} e^{-\frac{t}{\gamma}-\frac{t}{p(1-p)}} \\ &\quad + \frac{(1-2p)\sigma}{2p(1-p)^2}\int_0^t e^{-\frac{t-x}{\gamma}} \int_0^x e^{-\frac{x-y}{\gamma}-\frac{x-y}{p(1-p)}} dB_y dx \\ &\quad + \frac{\sigma}{2(1-p)}\int_0^t e^{-\frac{t-x}{\gamma}}(1-e^{-\frac{t-x}{p(1-p)}})dB_x \\ V_d &= \frac{\gamma\mu p+\gamma^2\mu}{p(1-p)+\gamma} - \gamma\mu e^{-\frac{t}{\gamma}} - \frac{p^2\gamma\mu}{p(1-p)+\gamma} e^{-\frac{t}{\gamma}-\frac{t}{p(1-p)}} \\ &\quad + \frac{(1-2p)\sigma}{2p(1-p)^2}\int_0^t e^{-\frac{t-x}{\gamma}} \int_0^x e^{-\frac{x-y}{\gamma}-\frac{x-y}{p(1-p)}} dB_y dx \\ &\quad + \frac{\sigma}{2(1-p)}\int_0^t e^{\frac{t-x}{\gamma}}(1+e^{-\frac{t-x}{p(1-p)}})dB_x \end{aligned} \tag{7.2}$$

Lemma 1 *By applying the martingale property of the integral* $\int_0^t f dB_t$ *for any measurable function* f*, we have the following identities*

$$\begin{cases} \langle V_s\rangle &= \frac{\mu\gamma^2}{p(1-p)+\gamma} - \mu\gamma e^{-\frac{t}{\gamma}} + \frac{\mu\gamma p(1-p)}{p(1-p)+\gamma} e^{-\frac{t}{\gamma}-\frac{t}{p(1-p)}} \\ \langle V_d\rangle &= \frac{\mu\gamma p+\mu\gamma^2}{p(1-p)+\gamma} - \mu\gamma e^{-\frac{t}{\gamma}} - \frac{\mu\gamma p^2}{p(1-p)+\gamma} e^{-\frac{t}{\gamma}-\frac{t}{p(1-p)}} \end{cases} \tag{7.3}$$

and

$$\begin{cases} \langle (V_s-\langle V_s\rangle)^2\rangle &= \frac{\sigma^2\gamma^3}{2[p(1-p)+\gamma][2p(1-p)+\gamma]} - \frac{\sigma^2\gamma}{2} e^{-\frac{2}{\gamma}t} \\ &\quad + \frac{2\sigma^2\gamma p(1-p)}{2p(1-p)+\gamma} e^{-\frac{2t}{\gamma}-\frac{t}{p(1-p)}} - \frac{\sigma^2\gamma p(1-p)}{2[p(1-p)+\gamma]} e^{-\frac{2t}{\gamma}-\frac{2t}{p(1-p)}} \\ \langle (V_d-\langle V_d\rangle)^2\rangle &= \frac{4\sigma^2\gamma^3(1-p)^2+8\sigma^2\gamma p^2(1-p)^2+4\sigma^2\gamma^2 p(1-p)(3-2p)}{8(1-p)^2[p(1-p)+\gamma][2p(1-p)+\gamma]} \\ &\quad - \frac{\sigma^2\gamma}{2} e^{-\frac{2}{\gamma}t} - \frac{2\sigma^2\gamma p^2}{2p(1-p)+\gamma} e^{-\frac{2t}{\gamma}-\frac{t}{p(1-p)}} \\ &\quad - \frac{\sigma^2\gamma p^3}{2(1-p)[p(1-p)+\gamma]} e^{-\frac{2t}{\gamma}-\frac{2t}{p(1-p)}} \end{cases} \tag{7.4}$$

8 Appendix B

Denote $V_s(t,p)$ and $V_d(t,p)$ as the solution of Eq. (3.3). We only consider the case of $p \to 0$. For any $t > 0$ the space $C[0,t]$ of all continuous functions on time interval $[0,t]$ is compact with the metrics $||x|| = \max_{[0,t]} |x(t)|$. Hence it suffices to prove that for any subsequence $V_s(t,p_n)$ and $V_d(t,p_n)$ with $\lim_{n\to\infty} p_n \to 0$, its limit is unique.

Multiplying both sides of the equation (3.3) for the somatic compartment by p_n and taking $p_n \to 0$, we see that $\lim_{n\to\infty} V_d(t, p_n) = \lim_{n\to\infty} V_s(t, p_n)$, provided that V_d and V_s are bounded. Now the equation for the dendritic compartment becomes

$$dV_d = g(V_s, V_d)dt + dI_{syn}(t) = g(V_d, V_d)dt + dI_{syn}(t) \tag{8.1}$$

and its solution is unique, under some reasonable conditions on g and I_{syn}. Hence for any sequence p_n with $p_n \to 0$ its limit $\lim_{n\to\infty} V_d(t, p_n) = \lim_{n\to\infty} V_s(t, p_n)$ is unique, satisfying Eq. (8.1). This completes our proof.

9 Appendix C

We first consider a diffusion process defined by

$$dX_t = \mu(X_t)dt + \sigma(X_t)dB_t \tag{9.1}$$

Let us introduce the following quantities

$$\begin{cases} s(x) &= \exp(-\int_0^x \dfrac{2\mu(y)}{\sigma^2(y)}dy) \\ m(x) &= \dfrac{1}{s(x)\sigma^2(x)} = \dfrac{\exp(\int_0^x \dfrac{2\mu(z)}{\sigma^2(z)}dz)}{\sigma^2(x)} \end{cases} \tag{9.2}$$

where m is the speed density, and s is the scale function. We say that a diffusion process is positive-recurrent if $\int_{-\infty}^{\infty} m(x)dx < \infty$ which is equivalent to $T < \infty$ where T is the first exit time of V_{thre}. For a positive-recurrent process, the stationary distribution density is given by $\pi(x) \sim m(x)$.

Theorem 1 *For a positive-recurrent diffusion process* X_t

$$\langle T \rangle = 2\int_{V_{rest}}^{V_{thre}} s(u)du \cdot \int_{-\infty}^{V_{rest}} m(u)du + 2\int_{V_{rest}}^{V_{thre}} (\int_y^{V_{thre}} s(u)du) \cdot m(y)dy \tag{9.3}$$

For $a \in I\!R$, let $G_{a,V_{thre}}(V_{rest}, y)\Delta y$ be the mean time spent in $(y, y + \Delta y)$ by the process X_t started at V_{rest} and run until it exits (a, V_{thre}). The expression for

$G_{a,V_{thre}}(V_{rest}, y)$ is given in [27] on page 198. Therefore we have

$$\langle T \rangle = \lim_{a \to -\infty} \int_a^{V_{thre}} G_{a,V_{thre}}(V_{rest}, y) dy$$

and Theorem 1 follows.